A Dramatic Steric Effect on the Rate of Migratory CO Insertion on Rhodium

Luca Gonsalvi,[†] Harry Adams,[†] Glenn J. Sunley,[‡] Evert Ditzel,[‡] and Anthony Haynes*[,†]

Department of Chemistry, University of Sheffield Sheffield, S3 7HF, UK
BP Chemicals Ltd
Hull Research and Technology Centre
Saltend, Hull HU12 8DS, UK

Received August 10, 1999

Ligand steric and electronic effects play a key role in determining organometallic reactivity trends and catalytic behavior. For monodentate ligands, a number of quantitative parameters (e.g. Tolman's cone angle[1]) are well-established concepts. Several important homogeneous catalysts now utilize bidentate ligands for which the stereoelectronic properties are less well understood.[2] Although the bidentate ligand "bite-angle" has been shown to be important,[3] understanding of the observed behavior at a molecular level is incomplete (as noted by Casey et al.[4]) and quantification of ligand effects on individual steps from catalytic cycles is quite rare. In this paper we report kinetic and crystallographic data which show that a subtle (but identifiable) steric interaction can have a dramatic influence on a key step in a catalytic carbonylation cycle.

Our results stem from an attempt to understand the 8-fold enhancement in catalytic activity recently reported for rhodium/iodide catalyzed methanol carbonylation utilizing the mixed P,S donor ligand, $Ph_2PCH_2P(S)Ph_2$ (dppms).[5] Strong donor ligands, particularly phosphines, are known to accelerate the rate determining oxidative addition of methyl iodide to Rh(I) and hence promote catalysis.[6] Our kinetic experiments show that while the dppms ligand gives the expected fast oxidative addition, it also promotes the subsequent CO insertion step (by a factor of ca. 3000 compared with $Ph_2PCH_2CH_2PPh_2$ (dppe)). Two X-ray crystal structures suggest that the conformation of the dppms phenyl groups results in steric congestion which accelerates CO insertion.

Scheme 1 shows a catalytic cycle for the dppms-promoted rhodium system based on preliminary mechanistic studies.[5b] It closely resembles the well-established cycle[7] for the original Monsanto catalyst, $[Rh(CO)_2I_2]^-$, and oxidative addition of MeI to [Rh(CO)I(dppms)] (**1a**) is thought to be rate determining. The stoichiometric reaction of **1a** with MeI (in the absence of CO) yields a stable acetyl product (**3a**) via a presumed methyl intermediate, **2a**. It is this reaction that we have studied in detail.

Scheme 1

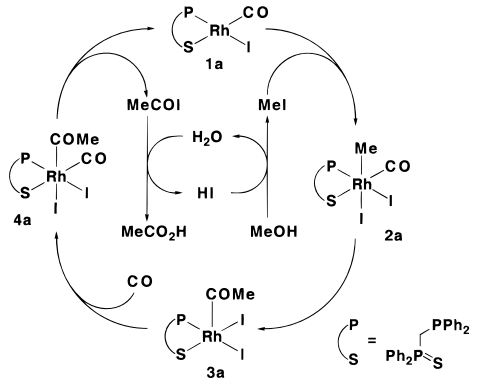

The reaction of **1a** with MeI, monitored by IR spectroscopy,[8] is first order in both [**1a**] and [MeI]. Kinetic data are given in Table 1. The activation parameters are typical for MeI addition, the large negative $\Delta S^{\ddagger}$ reflecting the highly ordered S_N2 transition state.[9] Extrapolation to 185 °C gives a predicted rate constant of 1.25 M^{-1} s^{-1} which is very close to that derived from catalytic rate data (2.16 M^{-1} s^{-1}),[10] confirming that oxidative addition of MeI to **1a** is rate determining for catalysis. Kinetic parameters measured for the analogous reaction of the diphosphine complex [Rh(CO)I(dppe)] (**1b**) are very similar (Table 1). Thus, addition of MeI to **1a** or **1b** is ca. 50 times faster at 25 °C than the corresponding reaction of $[Rh(CO)_2I_2]^-$ [11] but very similar to the rate reported recently for $[Rh(CO)I(PEt_3)_2]$.[6e]

Although the ligands dppms, dppe, and PEt_3 all promote MeI oxidative addition substantially, the resulting methyl complexes show dramatically different reactivity. With PEt_3 ligands, a stable, methyl product was isolated, which only undergoes methyl migration under CO pressure.[6e] In the dppe system, the intermediate $[MeRh(CO)I_2(dppe)]$ (**2b**) is relatively long-lived (half-life > 1 h) at room temperature.[6b] Kinetic parameters for migratory insertion in **2b** are reported in Table 1.

By contrast, migratory insertion in $[MeRh(CO)I_2(dppms)]$ (**2a**) is so fast that the intermediate was not previously detected.[5b] We have now obtained spectroscopic evidence for **2a** and an estimate for the CO insertion rate using the same approach used previously for $[MeRh(CO)_2I_3]^-$.[12] A series of IR spectra obtained during the reaction of **1a** with MeI at high concentration is shown in Figure 1. As well as the decay and appearance of strong ν(CO) bands due to **1a** and **3a** respectively, a very weak absorption is observed at higher frequency (2062 cm^{-1}) in exactly the region expected for **2a**.[13] This band decays in direct proportion to that of **1a** as predicted by the steady-state approximation. On the basis of observed IR absorbance and estimated extinction coefficient, we can estimate the ratio [**2a**]/[**1a**] and obtain the migratory insertion rate constant.[14] The value obtained (Table 1) is an order of magnitude larger than that found for $[MeRh(CO)_2I_3]^-$ (0.054 s^{-1}).

[†] Department of Chemistry, University of Sheffield.
[‡] BP Chemicals, Hull Research and Technology Centre.

(1) Tolman, C. A. *Chem. Rev.* **1977**, *77*, 313.
(2) (a) Landis, C. R.; Halpern, J. *J. Am. Chem. Soc.* **1987**, *109*, 1746. (b) Devon, T. J.; Phillips, G. W.; Puckette, T. A.; Stavinoha, J. L.; Vanderbilt, J. J. World Patent, WO87/07600, 1987. (c) Drent, E.; Budzelaar, P. H. M. *Chem. Rev.* **1996**, *96*, 663.
(3) Dierkes, P.; van Leeuwen, P. W. N. M. *J. Chem. Soc., Dalton Trans.* **1999**, 1519.
(4) Casey, C. P.; Paulsen, E. L.; Beuttenmueller, E. W.; Proft, B. R.; Petrovich, L. M.; Matter, B. A.; Powell, D. R. *J. Am. Chem. Soc.* **1997**, *119*, 11817.
(5) (a) Baker, M. J.; Dilworth, J. R.; Sunley, J. G.; Wheatley, N. European Patent Application, 632,006, 1995. (b) Baker, M. J.; Giles, M. F.; Orpen, A. G.; Taylor, M. J.; Watt, R. J. *J. Chem. Soc., Chem. Commun.* **1995**, 197.
(6) (a) Wegman, R. W.; Abatjoglou, A. G.; Harrison, A. M. *J. Chem. Soc., Chem. Commun.* **1987**, 1891. (b) Moloy, K. G.; Wegman, R. W. *Organometallics* **1989**, *8*, 2883. (c) Cavell, R. G. PCT Patent Application, WO 92/04118, 1992. (d) Dilworth, J. R.; Miller, J. R.; Wheatley, N.; Baker, M. J.; Sunley, J. G. *J. Chem. Soc., Chem. Commun.* **1995**, 1579. (e) Rankin, J.; Poole, A. D.; Benyei, A. C.; Cole-Hamilton, D. J. *Chem. Commun.* **1997**, 1835.
(7) (a) Forster, D. *Adv. Organomet. Chem.* **1979**, *17*, 255. (b) Dekleva, T. W.; Forster, D. *Adv. Catal.* **1986**, *34*, 81. (c) Maitlis, P. M.; Haynes, A.; Sunley, G. J.; Howard, M. J. *J. Chem. Soc., Dalton Trans.* **1996**, 2187.
(8) Reactions were monitored under pseudo-first-order conditions ([MeI] = 0.4−3.2 M) in a thermostated IR cell, following the ν(CO) bands of **1a** or **1b** at 1987 or 2011 cm^{-1} respectively.
(9) Griffin, T. R.; Cook, D. B.; Haynes, A.; Pearson, J. M.; Monti, D.; Morris, G. E. *J. Am. Chem. Soc.* **1996**, *118*, 3029.
(10) Calculated from the catalytic rate (19.6 M h^{-1}) reported in ref 5.
(11) Fulford, A.; Hickey, C. E.; Maitlis, P. M. *J. Organomet. Chem.* **1990**, *398*, 311.
(12) (a) Haynes, A.; Mann, B. E.; Gulliver, D. J.; Morris, G. E.; Maitlis, P. M. *J. Am. Chem. Soc.* **1991**, *113*, 8567. (b) Haynes, A.; Mann, B. E.; Morris, G. E.; Maitlis, P. M. *J. Am. Chem. Soc.* **1993**, *115*, 4093.
(13) The shift in ν(CO) between [M(CO)I(dppms)] and [MeM(CO)I_2-(dppms)] is 69 cm^{-1} for M = Rh, compared with 75 cm^{-1} for M = Ir.
(14) Assuming a two-step irreversible process **1a** → **2a** → **3a**, and applying the steady-state approximation to [**2a**], the ratio R = [**2a**]/[**1a**] = k_1[MeI]/k_2. Since $k_{obs} = k_1$[MeI], k_2 is given by the ratio k_{obs}/R. R was estimated based on the relative extinction coefficients observed for the stable Ir analogues.

10.1021/ja992891k CCC: $18.00
Published on Web 11/17/1999

Table 1. Rate Constants (25 °C, CH_2Cl_2) and Activation Paramters for Oxidative Addition and Migratory Insertion Reactions

reaction	rate constant	$\Delta H^{\ddagger}$/kJ mol^{-1}	$\Delta S^{\ddagger}$/J mol^{-1} K^{-1}
1a + MeI → **2a**	$1.19(5) \times 10^{-3}$ M^{-1} s^{-1}	47 ± 2	−144 ± 5
1b + MeI → **2b**	$1.41(5) \times 10^{-3}$ M^{-1} s^{-1}	40 ± 2	−167 ± 5
2a → **3a**	$6.2(10) \times 10^{-1}$ s^{-1}	54 ± 7	−67 ± 15
2b → **3b**	$1.6(1) \times 10^{-4}$ s^{-1}	83 ± 2	−38 ± 5

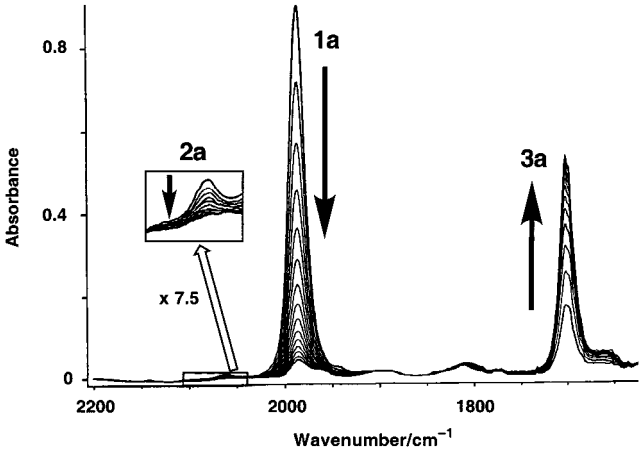

Figure 1. Series of IR spectra for the reaction of **1a** with MeI (8 M in CH_2Cl_2, 10 °C). Note the weak band due to intermediate **2a**.

[12b] Therefore *both* oxidative addition and migratory insertion steps in the reaction of **1a** with MeI are accelerated compared with the $[Rh(CO)_2I_2]^-$ system. Even more dramatic is the comparison in reactivity between dppms and dppe systems. At 25 °C the rate of migratory insertion is more than 3000 times faster for **2a** than for **2b**, corresponding to a lowering of $\Delta G^{\ddagger}_{298}$ by 20 kJ mol^{-1}.[15]

Electronic effects cannot account for the high reactivity of **2a**. Electron-donating ligands, while promoting oxidative addition, normally retard CO insertion, as for the dppe and PEt_3 systems. This can be partly explained by the formation of stronger Rh−Me bonds for the more nucleophilic precursors. Higher electron density on the metal also leads to stronger M(d) → CO(π*) back-bonding which is also thought to inhibit CO insertion.[16] In the case of the dppms system, the π-donor S atom trans to CO leads to even more pronounced back-donation, evidenced by the low ν(CO) frequency of **2a** (2062 cm^{-1}) compared with the dppe analogue (**2b**, 2076 cm^{-1}).

An explanation for the rapid migratory insertion in **2a** is suggested by X-ray crystallographic results. The model iridium methyl complex, $[MeIr(CO)I_2(dppms)]$ (**2c**), is the stable product of MeI oxidative addition to $[Ir(CO)I(dppms)]$ (**1c**).[17] The X-ray crystal structure[18] of **2c** (Figure 2) displays a pseudo-octahedral geometry with the methyl group occupying a position cis to both P and S donor atoms of the dppms ligand. The five-membered chelate ring adopts an envelope conformation that places two phenyl groups in axial positions creating a crowded "pocket" surrounding the methyl ligand. The adoption of this conformation is presumably due to the smaller cone angle of methyl (90°) compared with iodide (107°).[1] The closest contact between hydrogens of the phenyl and methyl groups is ca. 1.9 Å. This steric interaction causes the methyl ligand to lean away from the phenyl group, giving a P−Ir−Me bond angle of 96°.

An X-ray crystal structure[19] for the Rh acetyl complex **3a** (Figure 2) shows a distorted square-pyramidal geometry with the acetyl ligand in the apical site. The dppms ligand adopts a similar conformation to that in **2c** but now the axial phenyl substituents flank the vacant sixth coordination site. Thus the acetyl ligand in **3a** occupies a much less sterically demanding site than the methyl ligand in **2c**. We propose that migratory insertion in the Rh complex **2a** is accelerated by relief of the steric strain identified in the iridium model.

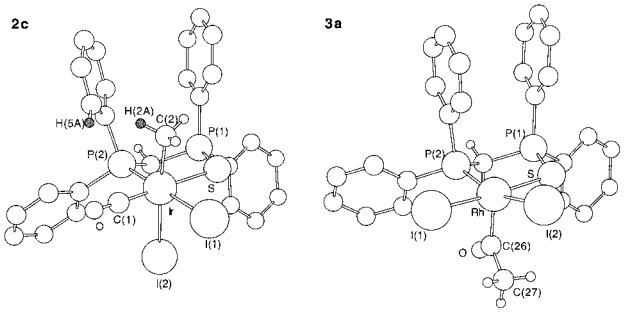

Figure 2. Molecular structures and numbering scheme for **2c** and **3a**. H atoms on the phenyl groups are removed for clarity (except H(5A) in **2c** to show the close contact with H(2A) of the methyl ligand).

A detailed conformational analysis has been reported previously for the five-membered rings in $M_2(\mu$-dppm) and M(dppe) complexes.[20] The $M_2(\mu$-dppm) ring is more rigid with greater constraints placed on the conformation of the phenyl substituents. Our M(dppms) chelate ring is analogous to an $M_2(\mu$-dppm) system, with a sulfur replacing one of the metal atoms, and similar conformational preferences might be expected in each case. We suggest that conformational rigidity in the dppms ligand leads to the steric interactions apparent in the structure of **2c** and causes the rapid migratory insertion in the Rh analogue **2a**.

In summary, our results show that electronic and steric effects of ligands can combine to give rather surprising and dramatic effects on the rates of key steps in catalytic cycles. By combining kinetic and crystallographic studies we have been able to quantify and understand these effects for two successive steps in a carbonylation process. Unusually, the dppms ligand is able to promote *both* oxidative addition and migratory insertion steps. The strong electron donation, which accelerates oxidative addition, would normally be expected to inhibit CO insertion, but this is overcome by a steric effect of the dppms ligand.

Acknowledgment. We thank BP Chemicals Ltd for financial support.

Supporting Information Available: Tables of kinetic data and details of X-ray crystal structures of **2c** and **3a** (PDF). This material is available free of charge via the Internet at http://pubs.acs.org.

JA992891K

(15) The rate of MeI oxidative addition to [Rh(CO)I(dppmo)] (dppmo = $Ph_2PCH_2P(O)Ph_2$) is very similar to that of complex **1a**. Migratory insertion is rapid but reversible, giving an equilibrium between methyl and acetyl complexes in CH_2Cl_2. Details will be included in a full paper.

(16) Margl, P.; Ziegler, T.; Blöchl, P. E. *J. Am. Chem. Soc.* **1996**, *118*, 5412.

(17) Complex **1c** was synthesized by the reaction of $Bu_4N[Ir(CO)_2I_2]$ with dppms in toluene/CH_2Cl_2. Selected spectroscopic data for new Ir compounds (all NMR spectra were recorded in CD_2Cl_2 and IR spectra in CH_2Cl_2): For **1c**: $^{31}P\{^1H\}$ δ(P) 25.8 (d), δ(P═S) 66.3 (d); ^2J(PP) 54 Hz; ν(CO) 1972 cm^{-1}. For **2c**: $^{31}P\{^1H\}$ δ(P) 18.7 (d), δ(P═S) 65.0 (d); ^2J(PP) 36 Hz; ^1H δ(CH_3Ir) 1.25 (d); ^3J(HP) 4 Hz; ν(CO) 2041 cm^{-1}.

(18) Crystal data (150 K) for **2c**: yellow; monoclinic; $P2_1/n$, a = 10.9897(13) Å, b = 14.0666(16) Å, c = 18.594(2) Å, β = 101.167(2)°; Z = 4, R_1 = 0.0272; wR_2 = 0.0539; GOF 1.110. Selected bond distances (Å) and angles (deg): Ir−C(1) 1.867(4), Ir−C(2) 2.143(5), Ir−P(2) 2.2923(10), Ir−S 2.4194(9), Ir−I(1) 2.7340(4), Ir−I(2) 2.7935(4), P(1)−S 2.0126(13), C(1)−Ir−C(2) 90.74(16), C(2)−Ir−P(2) 96.43 (11), C(2)−Ir−S 86.31(11), C(2)−Ir−I(1) 86.56(10), P(2)−Ir−S 91.32(3).

(19) Crystal data (293 K) for **3a**: yellow; monoclinic; $P2_1/c$, a = 13.125(13) Å, b = 13.234(16) Å, c = 16.642(18) Å, β = 94.23(3)°; Z = 4, R_1 = 0.0373; wR_2 = 0.0893; GOF 1.008. Selected bond distances (Å) and angles (deg): Rh−C(26) 1.951(6), Rh(1)−P(2) 2.256(2), Rh−S 2.357(2), Rh−I(1) 2.6497(19), Rh−I(2) 2.7024(19), P(1)−S 2.027(3), O−C(26) 1.178(7), C(26)−C(27) 1.491(9), C(26)−Rh−P(2) 92.80(19), C(26)−Rh−S 93.62(19), C(26)−Rh−I(1) 92.23(18), C(26)−Rh−I(2) 104.84(19), P(2)−Rh−S 90.47(9).

(20) Morton, D. A. V.; Orpen, A. G. *J. Chem. Soc., Dalton Trans.* **1992**, 641.